IEEE Access
Multidisciplinary | Rapid Review | Open Access Journal

Received November 21, 2019, accepted December 7, 2019, date of publication December 17, 2019,
date of current version January 14, 2020.

Digital Object Identifier 10.1109/ACCESS.2019.2960286

Impact of Imperfect Angle Estimation on Spatial and Directional Modulation

HONGYAN ZHANG[1], YUE XIAO[1], YANPING XIAO[1], AND WEI XIANG[2]
[1]National Key Laboratory of Science and Technology on Communications, University of Electronic Science and Technology of China, Chengdu 611731, China
[2]College of Science and Engineering, James Cook University, Cairns, QLD 4878, Australia

Corresponding author: Yue Xiao (xiaoyue@uestc.edu.cn)

This work was supported in part by the National Science Foundation of China under Grant 61671131, in part by the Fundamental Research Funds for the Central Universities under Grant ZYGX2018J092, and in part by the Sichuan Science and Technology Program under Grant 2018HH0138.

ABSTRACT In this paper, we investigate the impact of imperfect angle estimation (IAE) on spatial and directional modulation (SDM) systems, assuming that the signal experiences line of sight (LoS) propagation. In SDM systems with IAE, the variation is analyzed in detail, when there is a mismatch between the beamforming and precise channel matrices. Based on the union bound and statistics theory, the average bit error probabilities (ABEPs) for both the legitimate user and eavesdropper are derived. In addition, the ergodic rate is also quantified with IAE. Simulation results are presented to show that the achieved theoretical ABEPs are useful in quantifying the potential performance penalty. We also show that the mismatch between the beamforming and precise channel matrices will become greater with the increase in direction measurement error (DME), which affects the detection for both the legitimate user and eavesdropper. On the other hand, due to the effect of IAE, the SDM requires more signal-to-noise ratio (SNR) gain to achieve a stable ergodic secrecy rate.

INDEX TERMS Spatial and directional modulation, imperfect angle estimation, bit error rate, ergodic secrecy rate.

I. INTRODUCTION

Owing to the rapid development of 5G [1] and beyond 5G [2] wireless systems, the key communication technologies, such as massive multiple-input multiple-output (MIMO) [3], millimeter wave (mmWave) communications [4], unmanned aerial vehicles (UAVs) [5], satellite communications [6], and narrowband internet of things (NB-IoT) [7], desire to improve the security in addition to higher throughputs. Directional modulation (DM) [8]–[10], as a novel secure wireless transmission technique for 5G and IoT systems [11], [12], is capable of transmitting the modulated signal along a specified spatial direction, while scrambling the constellation formats of the signals in the other directions of line of sight (LoS) propagation.

There are a number of methods focusing on synthesizing DM signals and evaluating their performance [13]–[22]. More specially, previous works in [13]–[16] developed an analog DM architecture for synthesizing the modulated signals at the expense of implementation complexity, due to the process of designing constellation signals in the analog domain. Recently, for the sake of reducing the implementation complexity, DM baseband synthesis methods have been widely developed for the additive white Gaussian noise (AWGN) channel [17]–[22]. Particularly, in [20], the silent antenna hopping (SAH) technique was developed alongside a theoretical analysis of the bit error rate (BER) performance and security capacity in millimeter-wave communication systems. However, when the eavesdropper and legitimate user are located along the same direction, the security performance may be deteriorated. To address this issue, improved DM schemes with the aid of distributed receivers were developed [21], [22]. In [21], directional modulation with cooperative receivers was designed to prevent eavesdropping irrespective of the eavesdropper's direction, with only one data stream. Subsequently, spatial and directional modulation (SDM) with scrambling was considered in [22], where each modulated symbol is subjected to phase scrambling. Particularly, through combining spatial modulation (SM) [23]–[26] and DM, the resultant system is capable of offering higher

The associate editor coordinating the review of this manuscript and approving it for publication was Nan Wu.

spectral efficiency, in addition to an enhanced security performance. However, for SDM systems, the perfect angle knowledge is always assumed to be available at the transmitter, such that the impact of imperfect angle estimation (IAE) may be neglected in practical transmission condition.

In the literature, it is of prime significance to consider the impact of IAE, which has attracted considerable research interests in recent years (see [27]–[31] and references therein). More specially, some robust methods on designing the beamforming vector of the transmission signals and the projection matrix of the artificial noise have been widely investigated in the presence of the direction measurement error (DME) [28]–[31]. In [28], a closed-form expression for the artificial noise projection matrix was derived by assuming that DME is uniformly distributed in the single-desired-direction scenario. Subsequently, the authors of [29] considered a robust multibeam DM broadcasting system in various scenarios, where only one information stream can be transmitted to multiple legitimate users. To overcome this limitation, combining the main-lobe-intergration and leakage in the presence of DME was considered in [30], where multi-stream transmission is realized. Additionally, the authors of [31] proposed two novel schemes, which are capable of providing an improved secrecy sum-rate in the multicast scenario. Despite the influence of IAE has been studied in the aforementioned DM systems, it so far has not been considered for quantifying the performance of SDM systems.

In SM, although it is capable of transmitting information bitstream by the index of the activated antennas, it suffers from eavesdropping under the LoS channels. Meanwhile, DM has the ability to guarantee the transmission security, while the signals are modulated by traditional amplitude phase modulation (APM) symbols. By combing the advantage of SM and DM in the context of LoS channels, the SDM system not only inherits the benefit of high spectrum efficiency, but also achieves the information security. More specially, the authors of [24] considered the effect of channel estimation on SM systems, and the authors of [28]–[31] considered the effect of IAE on DM systems. However, the impact of IAE has not been evaluated for SDM systems. Therefore, in this paper, we study the effect of IAE on SDM systems in an LoS channel with a single antenna eavesdropper. The primary contributions of this paper can be summarized as follows:

1) We analyze the system model and digital transmitter architecture of SDM systems, with cooperative communications among multiple single-antenna receivers at the legitimate user. Specially, we introduce a scrambling factor into the beamforming vector for the sake of achieving DM characteristics. Subsequently, we take into account the impact of IAE during the whole transmission process, to quantify the performance degradation caused by the mismatch between the beamforming and precise channel matrices;
2) We derive the average bit error probability (ABEP) union-bounds for both the legitimate user and eavesdropper in the presence of DME, respectively. Furthermore, we provide the corresponding ergodic rates of both the legitimate user and eavesdropper as well as the ergodic secrecy rate of SDM systems. Our simulation results demonstrate that upon increasing the maximum value of DME, the mismatch between the beamforming matrix and the precise channel matrix increases, while the BER performance of the SDM decreases. On the other hand, when DME increases, the SDM needs more SNR gain to reach the upper bounds of the legitimate user's and eavesdropper's ergodic rates, respectively.

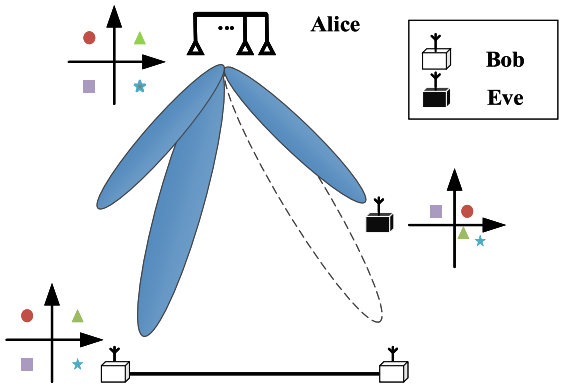

FIGURE 1. System model of SDM.

The remainder of this paper is organized as follows. In Section II, the SDM system is introduced alongside the SDM digital transmitter architecture described in detail. Section III presents the variation in the SDM system with IAE, where the beamforming and precise channel matrices do not match, which consequently results in uncertainty in detection at the legitimate user. Section IV analyzes both the ABEP union-bounds and ergodic rates associated with the legitimate user and the eavesdropper, as well as the system ergodic secrecy rate in the presence of DME. Simulation results are presented in Section V, while the concluding remarks are drawn in Section VI.

Notation: Throughout this paper, bold upper and lower case letters are used to represent matrices and vectors, respectively. In addition, $(\cdot)^H$, $Re(\cdot)$, $Im(\cdot)$, $\mathbb{E}(\cdot)$, $|\cdot|$, $\|\cdot\|$ refer to the conjugate transpose, real operation, imaginary operation, expectation operation, absolute value operation, and Frobenius norm, respectively. Furthermore, $p(\cdot)$, $Q(\cdot)$ and $\mathcal{CN}(\cdot,\cdot)$ are taken to mean the probability density function, Gaussian Q-function and circularly symmetric complex Gaussian distribution, respectively.

II. SPATIAL AND DIRECTIONAL MODULATION

We first introduce the system model of the SDM scheme, and then detail the digital transmitter architecture. Through designing the beamforming vector as the conjugate transpose of the precise channel vector, the SDM scheme enjoys a reduced detection complexity at the legitimate user.

A. SYSTEM MODEL

The simplified system model of SDM is depicted in Fig. 1, which consists of one N_t-element linear antenna array at the

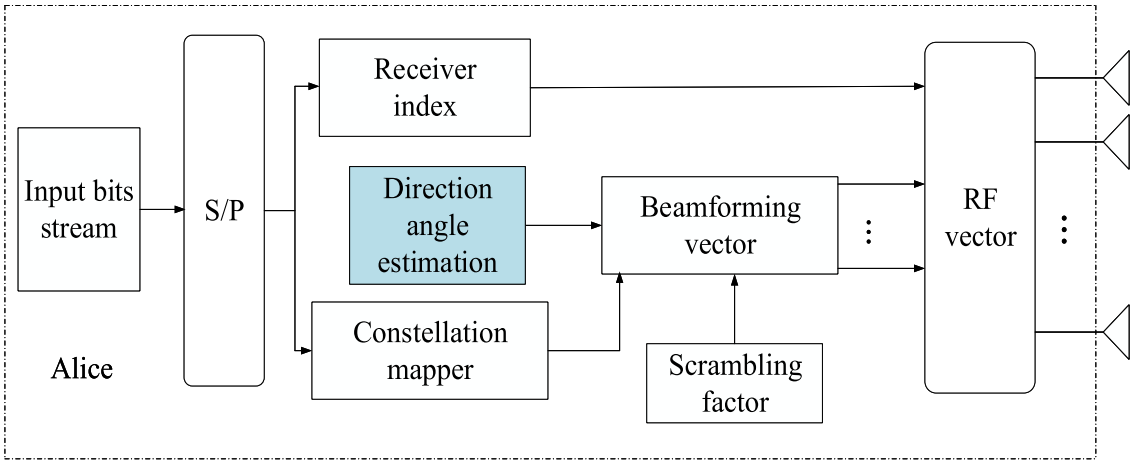

FIGURE 2. Digital transmitter architecture of SDM.

transmitter (Alice), N_r cooperative single-antenna receivers at the legitimate user (Bob) and a single antenna at the eavesdropper (Eve). For the sake of employing SM, it is assumed that N_r is the power of two, and these N_r cooperative single-antenna receivers are located in different spatial directions. Particularly, based on the concepts of SM and DM, Alice projects the modulated signal onto the selected receiver, as shown in Fig. 1, where the constellation signals can be correctly received at Bob, while the signals are scrambled at Eve.

In the SDM system, as the similar concepts of distributed antennas were proposed in [32]–[34], we assume that the N_r single-antenna receivers are connected by optical fibers, and Bob is equipped with a central unit. Particularly, in order to convert the radio frequency (RF) to/from digital intermediate frequency signal, each receiver is equipped with a transceiving device. When the digital intermediate frequency signals are obtained from receivers to Bob with the aid of optical fibers, the central unit is capable of facilitating a series of signal processings, such as the signal detection and demodulation.

B. DIGITAL TRANSMITTER ARCHITECTURE

The digital SDM transmitter architecture is depicted in Fig. 2. The SDM scheme, in addition to the employment of traditional M-ary APM, employs the indices of the receivers as an extra dimension to carry additional user signal information. Prior to transmission via the N_t-element linear antenna array, in accordance with part of input bitstream after the serial to parallel (S/P) conversion, APM symbols are obtained with the aid of the constellation mapper, while the indices of the receivers are attained by the remaining part of the bitstream. Note that the index activation pattern can be expressed by the N_r-dimensional standard basis vector. Additionally, the beamforming vector of the transmission signal is designed by the feedback of direction angle measurement and the introduction of the scrambling factor, and then the baseband signal is sent to the RF frontend. Similarly, it is noted that the receiver index is employed to determine which receiver of Bob is activated. More specially, since the scrambling factor is known at Bob but not at Eve, it offers the capability to improve system security. Meanwhile, as shown in Fig. 2, the accuracy of direction angle estimation has a significant effect on this system.

In the SDM system, there are total $\log_2(MN_r)$ bits in each transmission, where the first $\log_2(N_r)$ bits are modulated by the index of the activated receiver, while the other $\log_2(M)$ bits are modulated by conventional APM, such as phase shift keying (PSK) and quadrature amplitude modulation (QAM). Therefore, the SDM symbol vector can be expressed as

$$\mathbf{s}_i^m = \mathbf{e}_i b_m, \tag{1}$$

where $\mathbf{e}_i$ is the N_r-dimensional ith standard basis vector of the identity matrix $\mathbf{I}_{N_r \times N_r}$, which represents the ith activated receiver of Bob, and $b_m \in \mathcal{B} = \{b_1, b_2, \ldots, b_M\}$ is the APM symbol, which satisfies either the loose power constraint of $\mathbb{E}(|b_m|^2) = 1$ or the strict power constraint of $|b_m|^2 = 1$.

Particularly, in order to enhance the system security, a scrambling factor is introduced to the beamforming vector. After precoded by the beamforming matrix $\mathbf{W}$, the transmitted SDM signal vector in (1) passes through the LoS channel, and thus the received signal at any direction θ can be expressed as

$$\begin{aligned} y(\theta) &= \mathbf{h}^H(\theta)\,\mathbf{W}\mathbf{s}_i^m + n \\ &= \mathbf{h}^H(\theta)\,\mathbf{w}_i b_m + n, \end{aligned} \tag{2}$$

where n is the AWGN obeying $\mathcal{CN}\left(0, \sigma_n^2\right)$ with mean zero and variance σ_n^2. Furthermore, $\mathbf{h}^H(\theta)$ is the channel vector defined as

$$\mathbf{h}^H(\theta) = \left[e^{-jN_c L(\lambda,d,\theta)}, e^{-j(N_c-1)L(\lambda,d,\theta)}, \ldots, e^{jN_c L(\lambda,d,\theta)}\right], \tag{3}$$

where $N_c = \left(\frac{N_t-1}{2}\right)$ is the center of the antenna array, $L(\lambda, d, \theta) = \frac{2\pi}{\lambda} d\cos\theta$ is a function of the wavelength λ,

antenna spacing d at Alice, and direction θ at Bob. In particular, in order to avoid the creation of grating lobes, we assume $d \leq \lambda/2$. When considering all the receivers, the channel matrix between Alice and Bob is

$$\mathbf{H} = \left[\mathbf{h}(\theta_1), \mathbf{h}(\theta_2), \ldots, \mathbf{h}(\theta_{N_r})\right]^H, \tag{4}$$

where $\mathbf{H}$ satisfies $rank(\mathbf{H}) = N_r$ due to the power constraint. As can be seen from (2), in order to degrade the detection performance at Eve, the beamforming vector $\mathbf{w}_i$ for the ith receiver is designed as

$$\mathbf{w}_i = \alpha_i \mathbf{h}(\theta_i)/N_t, \tag{5}$$

where $\alpha_i = e^{j\varphi_i}$, $i = 1, \ldots, N_r$ is the scrambling factor that is known at Bob. Note that, in order to further enhance the security transmission, we update the scrambling factor at the symbol rate. In addition, when considering all the receivers, the beamforming matrix $\mathbf{W}$ is given by

$$\mathbf{W} = \left[\mathbf{w}_1, \mathbf{w}_2, \ldots, \mathbf{w}_{N_r}\right]. \tag{6}$$

Clearly, each element of $\mathbf{W}$ satisfies $\mathbf{h}^H(\theta_i)\,\mathbf{w}_i = \alpha_i$, $i \in [1, N_r]$. Hence, Eq. (2) in the desired direction θ_i simplifies

$$\begin{aligned} y(\theta_i) &= \mathbf{h}^H(\theta_i)\,\mathbf{W}\mathbf{s}_i^m + n \\ &= \mathbf{h}^H(\theta_i)\,\mathbf{w}_i b_m + n \\ &= \alpha_i b_m + n. \end{aligned} \tag{7}$$

Since Bob has the knowledge of α_i, the detection complexity is extremely reduced. However, it is usually difficult to achieve sufficient accuracy for the estimation of the directional angle, which consequently results in the mismatch between the beamforming vector and precise channel vector. Therefore, Eq. (2) cannot be further simplified.

III. IMPACT OF IAE ON SDM SYSTEMS

In this section, we investigate the SDM scheme with IAE. In practical SDM systems, it is impossible to attain the perfect angle information due to the noise and interference, so that the achievable performance of SDM with IAE will be degraded in comparison to its counterpart with perfect angle estimation.

A. ALICE'S TRANSMISSION

As aforementioned, for SDM with IAE, there always exists the distinct problem that one has to design the beamforming vector based on the estimated directional angle. The beamforming vector in (5) is given by

$$\widehat{\mathbf{w}}_i = \alpha_i \mathbf{h}(\widehat{\theta}_i)/N_t, \tag{8}$$

where $\widehat{\theta}_i$ is the estimated angle that differs from the perfect angle θ_i by DME $\Delta\theta_i$, namely $\widehat{\theta}_i = \theta_i + \Delta\theta_i$. For ease of exposition, it is assumed $\Delta\theta_i$ is approximately uniformly distributed over the interval of $[-\Delta\theta_m, \Delta\theta_m]$, and its probability density distribution is defined as

$$p(\Delta\theta_i) = \begin{cases} \dfrac{1}{2\Delta\theta_m}, & for\ -\Delta\theta_m \leq \Delta\theta_i \leq \Delta\theta_m \\ 0, & otherwise, \end{cases} \tag{9}$$

where $\Delta\theta_m$ is the maximum DME. When considering all the beamforming vectors, the beamforming matrix can be expressed as

$$\widehat{\mathbf{W}} = \left[\widehat{\mathbf{w}}_1, \widehat{\mathbf{w}}_2, \ldots, \widehat{\mathbf{w}}_{N_r}\right]. \tag{10}$$

After precoded by $\widehat{\mathbf{W}}$, the transmitted signal vector at Alice is

$$\mathbf{x} = \widehat{\mathbf{W}}\mathbf{s}_i^m = \widehat{\mathbf{w}}_i b_m. \tag{11}$$

Note that the beamforming vector in (8) does not match with the precise channel vector in the presence of DME. That is, the system does not satisfy $\mathbf{h}^H(\theta_i)\widehat{\mathbf{w}}_i = \alpha_i$, $i \in [1, N_r]$.

B. BOB'S DETECTION

The signal received at Bob can be written as

$$\begin{aligned} \mathbf{y}_B &= \mathbf{H}\mathbf{x} + \mathbf{n}_B \\ &= \mathbf{H}\widehat{\mathbf{W}}\mathbf{s}_i^m + \mathbf{n}_B, \end{aligned} \tag{12}$$

where $\mathbf{n}_B$ is the AWGN vector with $\mathbf{n}_B \sim \mathcal{CN}\left(0, \sigma_B^2 \mathbf{I}_{N_r \times 1}\right)$. Different from the SDM scheme with perfect angle knowledge, it is clear that (12) can't be further simplified, since the DME exists and can influence the design of the beamforming matrix.

Based on (12), joint detection of the activated receiver index i and the modulated APM symbol b_m follows the maximum likelihood (ML) criterion [35]. Hence, the ML detector can be obtained as

$$< \hat{i}, \hat{b}_m > = \arg \min_{i \in [1, N_r], b_m \in \mathcal{B}} ||\mathbf{y}_B - \widehat{\mathbf{H}}\widehat{\mathbf{W}}\mathbf{s}_i^m||^2, \tag{13}$$

where $\widehat{\mathbf{H}} = \left[\mathbf{h}(\widehat{\theta}_1), \mathbf{h}(\widehat{\theta}_2), \ldots, \mathbf{h}(\widehat{\theta}_{N_r})\right]^H$. It is noted that there are $N_r \cdot M$ Frobenius norms to be computed. For the sake of reducing the computational complexity, one may employ low-complexity near-ML (NML) detection, which treats the activated receiver index i and the modulated APM symbol b_m separately. Then the NML detector can be expressed as

$$\begin{aligned} \hat{i} &= \arg \min_{i \in [1, N_r]} \| |\mathbf{y}| - \mathbf{e}_i \|^2, \\ \hat{b}_m &= \arg \min_{b_m \in \mathcal{B}} \left\| \mathbf{y} - \alpha_{\hat{i}} \mathbf{e}_{\hat{i}} b_m \right\|^2. \end{aligned} \tag{14}$$

Thanks to the above process, one only needs to compute $N_r + M$ Frobenius norms.

In Fig. 3, the numbers of the Frobenius norm computations for ML and NML detection are shown. Compared to joint ML detection, NML detection offers a reduced computational complexity, especially when the number of the receivers and the modulation order are large. Nevertheless, DME leads to a potential performance penalty.

C. EVE'S DETECTION

The signal received at Eve can be written as

$$\begin{aligned} z &= \mathbf{h}^H(\theta_E)\mathbf{x} + n_E \\ &= \mathbf{h}^H(\theta_E)\widehat{\mathbf{W}}\mathbf{s}_i^m + n_E, \end{aligned} \tag{15}$$

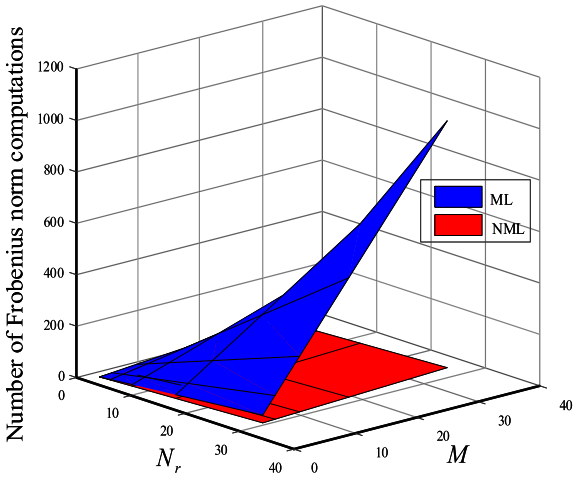

FIGURE 3. Complexity comparison between ML and NML detection.

where θ_E is Eve's direction, n_E is the AWGN with a distribution of $\mathcal{CN}\left(0, \sigma_E^2\right)$. Since the channel state information (CSI) between Alice and Bob cannot be obtained at Eve, when the scrambling factor is introduced to the beamforming matrix, Eve may employ ML detection to obtain the modulated APM symbol b_m as

$$\hat{b}_m = \arg \min_{b_m \in \mathcal{B}} \|z - b_m\|^2. \tag{16}$$

Due to the introduction of SM, only one receiver is activated in each transmission. Therefore, it is difficult to recover this part of information modulated by the receiver index, since Eve cannot exactly know which receiver of Bob is activated. On the other hand, Eq. (16) shows that the detection performance of b_m is degraded attributed to the beamforming matrix. Even in the worst scenario that Eve has perfect knowledge of the CSI between Alice and Bob, the correct information is still difficult to be recovered due to the presence of the scrambling factor and DME. Thus, it can be concluded that the performance of the SDM scheme with IAE is prohibitively poor.

IV. PERFORMANCE ANALYSIS

In this section, in the context of DME, we aim to derive the ABEP bounds and ergodic rates of Bob and Eve, as well as qualify the ergodic secrecy rate of the SDM system.

A. BER PERFORMANCE ANALYSIS

Under the assumption of ML detection, the ABEP union bounds of Bob and Eve are obtained. Based on [22], we extend the derivation of the ABEP union bound to the scenario where the DME is present.

1) AVERAGE BER OF BOB

Base on the joint ML detection in (13), the ABEP union bound of Bob can be obtained as

$$P_B \leq \frac{1}{|S| \log_2(|S|)} \times \sum_{\mathbf{s}_i^m \in S} \sum_{\mathbf{s}_j^n \in S} e(\mathbf{s}_i^m, \mathbf{s}_j^n) \mathbb{E}_{\Delta\Theta}\{P(\mathbf{s}_i^m \to \mathbf{s}_j^n | \Delta\Theta)\}, \tag{17}$$

where S is the alphabet of the SDM symbol vector, $e(\mathbf{s}_i^m, \mathbf{s}_j^n)$ denotes the Hamming distance between the equivalent bit representations of $\mathbf{s}_i^m$ and $\mathbf{s}_j^n$, and $\Delta\Theta = [\Delta\theta_1, \Delta\theta_2, \ldots, \Delta\theta_{N_r}]$ represents Bob's DME vector. Furthermore, $\mathbb{E}_{\Delta\Theta}\{P(\mathbf{s}_i^m \to \mathbf{s}_j^n | \Delta\Theta)\}$ is the conditional average pairwise error probability (APEP), where each element of $\Delta\Theta$ obeys a uniform distribution.

Particularly, the APEP is given in (18), which is shown at the bottom of this page and where $Re\left\{\left(\widehat{\mathbf{H}}\widehat{\mathbf{W}}\mathbf{s}_j^n - \widehat{\mathbf{H}}\widehat{\mathbf{W}}\mathbf{s}_i^m\right)\mathbf{n}_B{}^H\right\}$ is the AWGN, which obeys $\mathcal{CN}\left(0, \frac{\sigma_B^2}{2}\left\|\widehat{\mathbf{H}}\widehat{\mathbf{W}}s_j^n - \widehat{\mathbf{H}}\widehat{\mathbf{W}}\mathbf{s}_i^m\right\|^2\right)$. Consequently, the APEP in (18), as shown at the bottom of this page, reduces to

$$P(\mathbf{s}_i^m \to \mathbf{s}_j^n | \Delta\Theta) = Q\left(\frac{\left\|\mathbf{H}\widehat{\mathbf{W}}\mathbf{s}_i^m - \widehat{\mathbf{H}}\widehat{\mathbf{W}}\mathbf{s}_j^n\right\|^2 - \left\|\mathbf{H}\widehat{\mathbf{W}}\mathbf{s}_i^m - \widehat{\mathbf{H}}\widehat{\mathbf{W}}\mathbf{s}_i^m\right\|^2}{\sqrt{2}\sigma_B\left\|\widehat{\mathbf{H}}\widehat{\mathbf{W}}\mathbf{s}_i^m - \widehat{\mathbf{H}}\widehat{\mathbf{W}}\mathbf{s}_j^n\right\|}\right). \tag{19}$$

$$\begin{aligned}
&P\left(\mathbf{s}_i^m \to \mathbf{s}_j^n | \Delta\Theta\right) \\
&= P\left(\left\|\mathbf{y}_B - \widehat{\mathbf{H}}\widehat{\mathbf{W}}\mathbf{s}_i^m\right\|^2 > \left\|\mathbf{y}_B - \widehat{\mathbf{H}}\widehat{\mathbf{W}}\mathbf{s}_j^n\right\|^2\right) \\
&= P\left\{\left(\mathbf{H}\widehat{\mathbf{W}}s_i^m - \widehat{\mathbf{H}}\widehat{\mathbf{W}}\mathbf{s}_i^m + \mathbf{n}_B\right)^H \left(\mathbf{H}\widehat{\mathbf{W}}s_i^m - \widehat{\mathbf{H}}\widehat{\mathbf{W}}\mathbf{s}_i^m + \mathbf{n}_B\right) > \left(\mathbf{H}\widehat{\mathbf{W}}\mathbf{s}_i^m - \widehat{\mathbf{H}}\widehat{\mathbf{W}}\mathbf{s}_j^n + \mathbf{n}_B\right)^H \left(\mathbf{H}\widehat{\mathbf{W}}\mathbf{s}_i^m - \widehat{\mathbf{H}}\widehat{\mathbf{W}}\mathbf{s}_j^n + \mathbf{n}_B\right)\right\} \\
&= P\left\{\left\|\mathbf{H}\widehat{\mathbf{W}}\mathbf{s}_i^m - \widehat{\mathbf{H}}\widehat{\mathbf{W}}\mathbf{s}_i^m\right\|^2 + 2Re\left\{\left(\mathbf{H}\widehat{\mathbf{W}}\mathbf{s}_i^m - \widehat{\mathbf{H}}\widehat{\mathbf{W}}\mathbf{s}_i^m\right)\mathbf{n}_B{}^H\right\} > \left\|\mathbf{H}\widehat{\mathbf{W}}\mathbf{s}_i^m - \widehat{\mathbf{H}}\widehat{\mathbf{W}}\mathbf{s}_j^n\right\|^2 + 2Re\left\{\left(\mathbf{H}\widehat{\mathbf{W}}\mathbf{s}_i^m - \widehat{\mathbf{H}}\widehat{\mathbf{W}}\mathbf{s}_j^n\right)\mathbf{n}_B{}^H\right\}\right\} \\
&= P\left\{2Re\left\{\left(\widehat{\mathbf{H}}\widehat{\mathbf{W}}\mathbf{s}_j^n - \widehat{\mathbf{H}}\widehat{\mathbf{W}}\mathbf{s}_i^m\right)\mathbf{n}_B{}^H\right\} > \left\|\mathbf{H}\widehat{\mathbf{W}}\mathbf{s}_i^m - \widehat{\mathbf{H}}\widehat{\mathbf{W}}\mathbf{s}_j^n\right\|^2 - \left\|\mathbf{H}\widehat{\mathbf{W}}\mathbf{s}_i^m - \widehat{\mathbf{H}}\widehat{\mathbf{W}}\mathbf{s}_i^m\right\|^2\right\} \\
&= P\left\{Re\left\{\left(\widehat{\mathbf{H}}\widehat{\mathbf{W}}\mathbf{s}_j^n - \widehat{\mathbf{H}}\widehat{\mathbf{W}}\mathbf{s}_i^m\right)\mathbf{n}_B{}^H\right\} > \frac{\left\|\mathbf{H}\widehat{\mathbf{W}}\mathbf{s}_i^m - \widehat{\mathbf{H}}\widehat{\mathbf{W}}\mathbf{s}_j^n\right\|^2 - \left\|\mathbf{H}\widehat{\mathbf{W}}\mathbf{s}_i^m - \widehat{\mathbf{H}}\widehat{\mathbf{W}}\mathbf{s}_i^m\right\|^2}{2}\right\}
\end{aligned} \tag{18}$$

Furthermore, according to [21], when the number of N_t is large enough, we have $\mathbf{h}^H(\theta_k)\widehat{\mathbf{w}}_i \approx 0$, $k \neq i$, and $\widehat{\mathbf{H}}\widehat{\mathbf{W}} \approx \mathbf{I}_{N_r}$. Thus, the APEP of (19) can be expressed as

$$\begin{aligned} &P(\mathbf{s}_i^m \to \mathbf{s}_j^n|\Delta\Theta) \\ &\approx Q\left(\frac{\left\|\mathbf{R}\mathbf{s}_i^m - \mathbf{s}_j^n\right\|^2 - \left\|\mathbf{R}\mathbf{s}_i^m - \mathbf{s}_i^m\right\|^2}{\sqrt{2}\sigma_B\left\|\mathbf{s}_i^m - \mathbf{s}_j^n\right\|}\right) \\ &= Q\left(\frac{\left\|\mathbf{e}_i r_i b_m - \mathbf{e}_j b_n\right\|^2 - \left\|\mathbf{e}_i r_i b_m - \mathbf{e}_i b_m\right\|^2}{\sqrt{2}\sigma_B\left\|\mathbf{e}_i b_m - \mathbf{e}_j b_n\right\|}\right) \\ &= \begin{cases} Q\left(\dfrac{|r_i b_m - b_n|^2 - |r_i - 1|^2}{\sqrt{2}\sigma_B|b_m - b_n|}\right), & i = j \\ Q\left(\dfrac{|r_i|^2 + 1 - |r_i - 1|^2}{2\sigma_B}\right), & i \neq j \end{cases} \\ &= \begin{cases} Q\left(\dfrac{2Re\left\{r_i\left(1 - b_m b_n^H\right)\right\}}{\sqrt{2}\sigma_B|b_m - b_n|}\right), & i = j \\ Q\left(\dfrac{Re\{r_i\}}{\sigma_B}\right), & i \neq j, \end{cases} \end{aligned} \tag{20}$$

where $\mathbf{R} = diag\left(r_1, r_2, \ldots, r_{N_r}\right)$, and $r_i = \mathbf{h}^H(\theta_i)\,\widehat{\mathbf{w}}_i$. Note that in the SDM system, the precise channel vector $\mathbf{h}^H(\theta_i)$ is not known due to the presence of DME. However, there is a certain reference value for the implementation in practical scenarios, when the theoretical analysis is employed.

2) AVERAGE BER OF EVE

In this part, the ABEP union bound of Eve is obtained. The user information is modulated by the index of cooperative receiver, in addition to traditional APM symbols. Thus, the ABEP union bound of Eve can be derived in the following two steps.

Firstly, similar to (17), the analytical ABEP of the APM symbols is given by

$$P_M \leq \frac{1}{M\log_2 M} \times \sum_{m=1}^{M}\sum_{n=1}^{M} e\left(b_m, b_n\right)\mathbb{E}_{\Delta\Theta}\{P(b_m \to b_n)|\Delta\Theta\}, \tag{21}$$

where $e(b_m, b_n)$ is the Hamming distance between the equivalent bit representations of b_m and b_n, and $\mathbb{E}_{\Delta\Theta}\{P(b_m \to b_n)|\Delta\Theta\}$ is the conditional APEP. Moreover, according to [22], the conditional APEP can be given by

$$\mathbb{E}_{\Delta\Theta}\{P(b_m \to b_n)|\Delta\Theta\} = \frac{1}{N_r}\sum_{i=1}^{N_r}\mathbb{E}_{\Delta\theta_i}\{P(b_m \to b_n|\Delta\theta_i)\}, \tag{22}$$

where $\mathbb{E}_{\Delta\theta_i}\{P(b_m \to b_n)|\Delta\theta_i\}$ is also the conditional APEP, which represents that the ith legitimate receiver is activated. Furthermore, the conditional APEP can be derived as

$$\begin{aligned} &\mathbb{E}_{\Delta\theta_i}\{P(b_m \to b_n)|\Delta\theta_i\} \\ &= \mathbb{E}_{\Delta\theta_i}\left\{Q\left(\frac{u_n\widehat{R}_{i,m}}{\sqrt{\sigma_E^2/2}}\right)Q\left(\frac{v_n\widehat{I}_{i,m}}{\sqrt{\sigma_E^2/2}}\right)\right\}, \end{aligned} \tag{23}$$

where $u_n = \begin{cases} 1, n = 2, 3 \\ -1, n = 1, 4 \end{cases}$ and $v_n = \begin{cases} 1, n = 3, 4 \\ -1, n = 1, 2 \end{cases}$. $\widehat{R}_{i,m}$ and $\widehat{I}_{i,m}$ respectively are the real and imaginary parts of received noiseless signal (defined as z_n) at Eve. That is, z_n can be written as

$$\begin{aligned} z_n &= \mathbf{h}^H(\theta_E)\widehat{\mathbf{W}}\mathbf{s}_i^m \\ &= \widehat{R}_{i,m} + j\widehat{I}_{i,m}. \end{aligned} \tag{24}$$

Secondly, owing to the special architecture of SM, Eve cannot determine which receiver of Bob is activated, and thus we assume that the ABEP of the receiver index is 1/2.

Consequently, based on the above two steps, while considering the expectation operation, the ABEP union bound of Eve can be given by (25), as shown at the bottom of this page.

B. ERGODIC RATE ANALYSIS

In this subsection, we investigate the performance of SDM in an ergodic-rate sense to measure the secrecy performance, when the ML detections of (13) and of (16) are employed. According to [36], the ergodic secrecy rate is the difference between the ergodic rates of Bob and Eve as

$$R_{\text{sec}} = [R_B - R_E]^+, \tag{26}$$

where $[x]^+ = \max\{0, x\}$, R_B and R_E respectively, as the ergodic rates of Bob and Eve.

Since the SDM system is special in the sense that its input symbol vector $\mathbf{s}_i^m$ consists of the finite-alphabet receiver index and APM symbol. In other words, $\mathbf{s}_i^m$ is discrete, while the output y is continuous. This implies that the considered channel is discrete-input continuous-output memoryless channel. Based on [37], [38], Bob's ergodic rate can be written as

$$\begin{aligned} R_B &= \log(MN_r) \\ &\quad - \frac{1}{MN_r}\sum_{i=1}^{N_r}\sum_{m=1}^{M}\mathbb{E}_{\Delta\Theta,\mathbf{n}_B}\left[\log_2\sum_{j=1}^{N_r}\sum_{n=1}^{M}\exp\left(\Psi\right)\right], \end{aligned} \tag{27}$$

$$P_z \leq \frac{\log_2 M}{\log_2(MN_r)} \times \underbrace{\frac{1}{MN_r\log_2 M}\sum_{i=1}^{N_r}\sum_{m=1}^{M}\sum_{n=1}^{M} e(b_m, b_n)\mathbb{E}_{\Delta\theta_i}\left\{Q\left(\frac{u_n\widehat{R}_{i,m}}{\sqrt{\sigma_E^2/2}}\right)Q\left(\frac{v_n\widehat{I}_{i,m}}{\sqrt{\sigma_E^2/2}}\right)\right\}}_{ABEP\ of\ APM\ symbol} + \frac{\log_2 N_r}{\log_2(MN_r)} \times \frac{1}{2} \tag{25}$$

where Ψ is formulated as

$$\Psi = \frac{-\left\|\mathbf{H}\widehat{\mathbf{W}}\left(\mathbf{s}_i^m - \mathbf{s}_j^n\right) + \mathbf{n}_B\right\|^2 + \|\mathbf{n}_B\|^2}{\sigma_B^2}. \quad (28)$$

Observing that $\Psi = 0$ when $i = j$ and $m = n$, (27) can be rewritten as

$$R_B = \log(MN_r) - \frac{1}{MN_r}\sum_{i=1}^{N_r}\sum_{m=1}^{M}\mathbb{E}_{\Delta\Theta,\mathbf{n}_B}\left[\log_2\sum_{\substack{j=1\\ j\neq i}}^{N_r}\sum_{\substack{n=1\\ n\neq m}}^{M}(1+\exp(\Psi))\right]. \quad (29)$$

Note that, denote the signal-to-noise ratio (SNR) by $SNR = 1/\sigma_B^2$, when $SNR \to \infty$, the $\exp(\Psi) \to 0$, so we can attain Bob's ergodic rate upper bound as $\log_2(MN_r)$.

On the other hand, as aforementioned, Eve can not determine which receiver of Bob is activated, only can recover the part of information transmitted by APM symbols. Thus, when we consider Bob's ith receiver is activated, similar to (29), Eve's ergodic rate can be written as

$$R_E = \log_2 M - \frac{1}{M}\sum_{m=1}^{M}\mathbb{E}_{\Delta\theta_i,n_E}\left[\log_2\sum_{\substack{n=1\\ n\neq m}}^{M}(1+\exp(\Phi))\right], \quad (30)$$

where Φ is given by

$$\Phi = \frac{-\left\|\mathbf{h}^H(\theta_E)\,\widehat{\mathbf{w}}_i(b_m - b_n) + n_E\right\|^2 + \|n_E\|^2}{\sigma_E^2}. \quad (31)$$

When considering all the receivers of Bob, (30) is simplified to

$$R_E = \log_2 M - \frac{1}{MN_r}\sum_{i=1}^{N_r}\sum_{m=1}^{M}\mathbb{E}_{\Delta\theta_i,n_E}\left[\log_2\sum_{\substack{n=1\\ n\neq m}}^{M}(1+\exp(\Phi))\right]. \quad (32)$$

Assuming $\sigma_E^2 = \sigma_B^2$, obviously, Eve can reach ergodic rate upper bound of $\log_2 M$, when $SNR \to \infty$.

Consequently, upon substituting (29) and (32) into (26), the ergodic secrecy rate of the SDM system can be obtain as

$$R_{\text{sec}} = \left\{\log_2 N_r - \frac{1}{MN_r}\sum_{i=1}^{N_r}\sum_{m=1}^{M}\mathbb{E}_{\Delta\Theta,\mathbf{n}_B,n_E}\log_2(\Gamma)\right\}^+, \quad (33)$$

where Γ is given by

$$\Gamma = \frac{\sum_{\substack{j=1\\ j\neq i}}^{N_r}\sum_{\substack{n=1\\ n\neq m}}^{M}(1+\exp(\Psi))}{\sum_{\substack{n=1\\ n\neq m}}^{M}(1+\exp(\Phi))}. \quad (34)$$

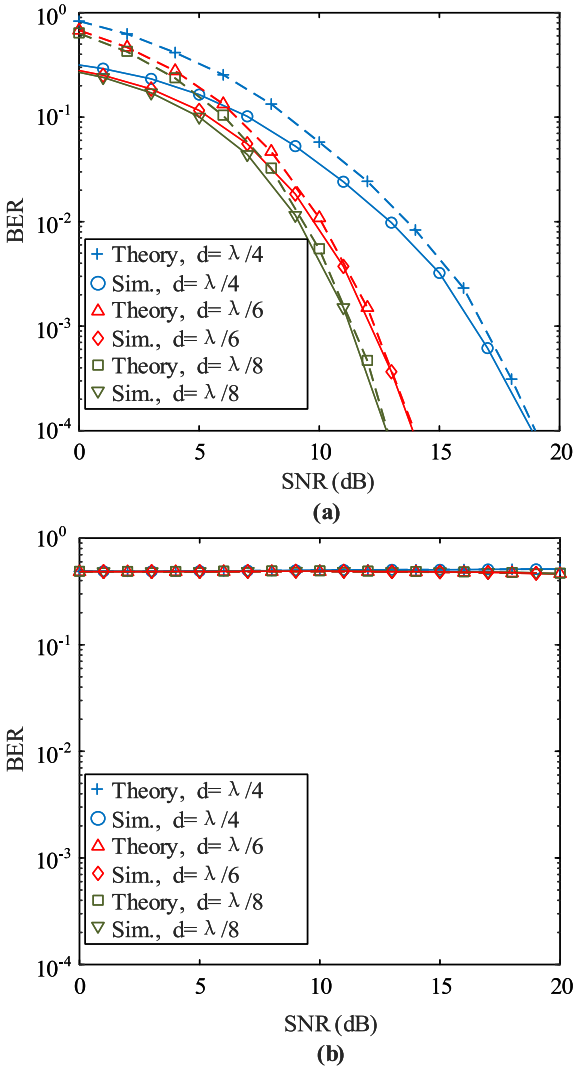

FIGURE 4. Theoretical and simulated BERs for different antenna spacing d with the maximum DME 6°. (a) Bob's BER versus the SNR; (b) Eve's BER versus the SNR.

Particularly, when $SNR \to \infty$, the ergodic secrecy rate tends to $\log_2 N_r$.

V. SIMULATION RESULTS AND ANALYSIS

In this section, we provide our simulation results in an attempt to demonstrate the impact of IAE on the SDM system employing $N_t = 32$ antennas at Alice and single antenna at Eve in the context of LoS channels. By comparison, the conventional SAH scheme [20] and the SDM scheme without DME ($\Delta\theta_m = 0$) are considered. Moreover, in our simulation results, we employ ML detection of (13) at Bob and of (16) at Eve, and the other parameters are listed in Table 1, where Λ is the scrambling factor set. Furthermore, as mentioned in Section IV-B, we assume $\sigma_B^2 = \sigma_E^2$ and set the SNR as $1/\sigma_B^2$.

A. ACHIEVABLE BER

Fig. 4 presents the achievable BER performance versus the SNR for different antenna spacing d, where both the

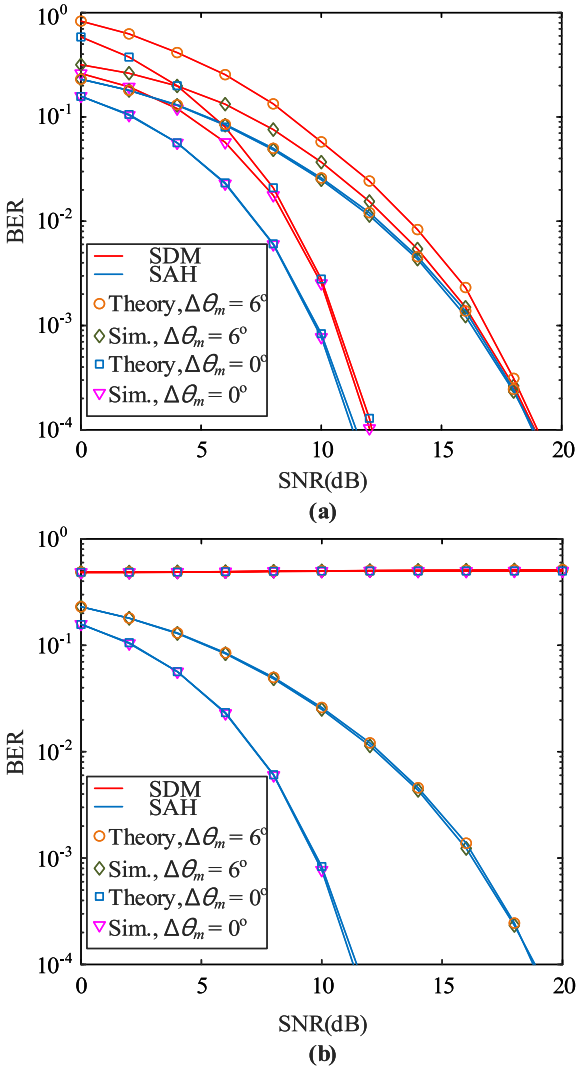

FIGURE 5. BER performances of both the SDM and conventional SAH schemes with and without DME. (a) Bob's BER versus the SNR; (b) Eve's BER versus the SNR.

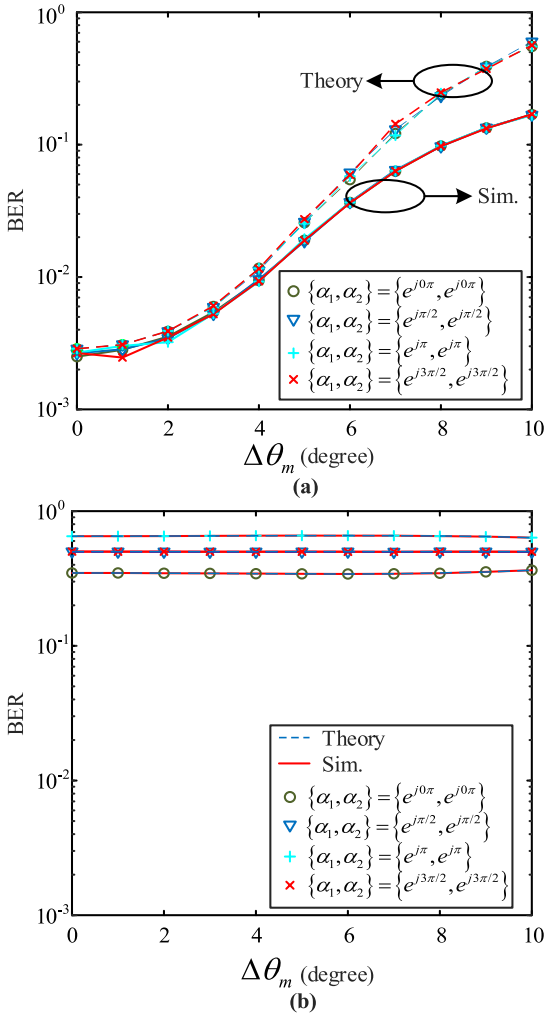

FIGURE 6. BER performances of the SDM scheme with a variety of scrambling factor sets. (a) Bob's BER versus the the maximum DME; (b) Eve's BER versus the maximum DME.

theoretical and simulated results are given. As can be observed in Fig. 4(a), at a given SNR, the BER of Bob decreases with the decrease of d. By contrast, in Fig. 4(b), Eve's BER curves with $d = \lambda/8, \lambda/6, \lambda/4$ are nearly identical over the entire SNR region. Furthermore, it is noted that the theoretical results of Bob in (17) and Eve in (25) form tight upper bounds of the simulated results in the entire SNR region, when DME is sufficiently high. These observations show that the derivations in Section IV-A are valid, and the theoretical results concerning IAE provide certain reference for the implementation in practical scenarios, especially in the high SNR region.

Fig. 5 compares the theoretical and simulated BER performance versus the SNR for both the SDM and SAH schemes, when assuming $\theta_E = 135°$ in the SAH scheme. Fig. 5(a) shows that Bob's BER performance in both SDM and SAH with DME is worse than those without DME, and the performance gap becomes significant, when SNR increases. Note that, at a given DME, for higher SNR, the performance gap between theoretical and simulated results of the SAH scheme can be negligible and that of the SDM scheme gradually becomes smaller. On the other hand, as can be seen from Fig. 5(b), Eve's BER in the SAH scheme exhibits a similar performance to that of Bob. By contrast, Eve's BER performance in SDM is sufficiently degraded in the entire DME region. This is owing to the fact that for the SDM scheme, Eve is not aware of the scrambling factor, and does not know which receiver of Bob is activated.

Fig. 6 depicts the theoretical and simulated BER versus the maximum DME for a variety of scrambling factor sets $\{\alpha_1, \alpha_2\}$, where SNR is fixed to 10 dB. As can be observed from Fig. 6(a), the gap between Bob's theoretical and simulated results becomes large for low SNR, and Bob's BER performance degrades for a given set of scrambling factors, when the maximum $\Delta\theta_m$ increases. In addition to our observation with respect to $\Delta\theta_m$, it is difficult to discern the curves for different scrambling factor sets. In other words, the effect of the scrambling factor on Bob's BER performance

TABLE 1. System parameters.

Fig.	Scheme	λ	N_r	M	$\theta_i, i = 1, \ldots, N_r$	Λ	θ_E	$\Delta\theta_m$	SNR
4	SDM	$\lambda/8, \lambda/6, \lambda/4$	2	4	$60°, 135°$	$\{e^{j\pi/6}, e^{j4\pi/9}\}$	135°	6°	-
5	SDM	$\lambda/4$	2	4	$60°, 135°$	$\{e^{j\pi/6}, e^{j4\pi/9}\}$	135°	$0°, 6°$	10dB
	SAH	$\lambda/4$	1	4	135°	-	135°	$0°, 6°$	10dB
6	SDM	$\lambda/4$	2	4	$60°, 135°$	$\{e^{j0\pi}, e^{j0\pi}\}, \{e^{j\pi/2}, e^{j\pi/2}\}, \{e^{j\pi}, e^{j\pi}\}, \{e^{j3\pi/2}, e^{j3\pi/2}\}$	135°	-	10dB
7	SDM	$\lambda/4$	2	4	$60°, 135°$	$\{e^{j\pi/6}, e^{j4\pi/9}\}$	-	$0°, 6°$	10dB
	SAH	$\lambda/4$	1	4	135°	-	-	$0°, 6°$	10dB
8	SDM	$\lambda/4$	2	4	$60°, 135°$	$\{e^{j\pi/6}, e^{j4\pi/9}\}$	-	$0°, 6°$	10dB
9	SDM	$\lambda/4$	2	4	$60°, 135°$	$\{e^{j\pi/6}, e^{j4\pi/9}\}$	135°	$0°, 3°, 6°$	-
10	SDM	$\lambda/4$	2	4	$60°, 135°$	$\{e^{j\pi/6}, e^{j4\pi/9}\}$	135°	6°	-
		$\lambda/4$	4	4	$20°, 60°, 135°, 170°$	$\{e^{j\pi/12}, e^{j\pi/6}, e^{j4\pi/9}, e^{j2\pi/3}\}$	135°	6°	-
		$\lambda/4$	8	4	$5°, 25°, 40°, 60°, 80°, 100°, 135°, 160°$	$\{e^{j\pi/36}, e^{j\pi/12}, e^{j\pi/6}, e^{j2\pi/9}, e^{j13\pi/45}, e^{j4\pi/9}, e^{j2\pi/3}, e^{j29\pi/45}\}$	135°	6°	-
11	SDM	$\lambda/4$	2	4,16,64	$60°, 135°$	$\{e^{j\pi/6}, e^{j4\pi/9}\}$	135°	6°	-

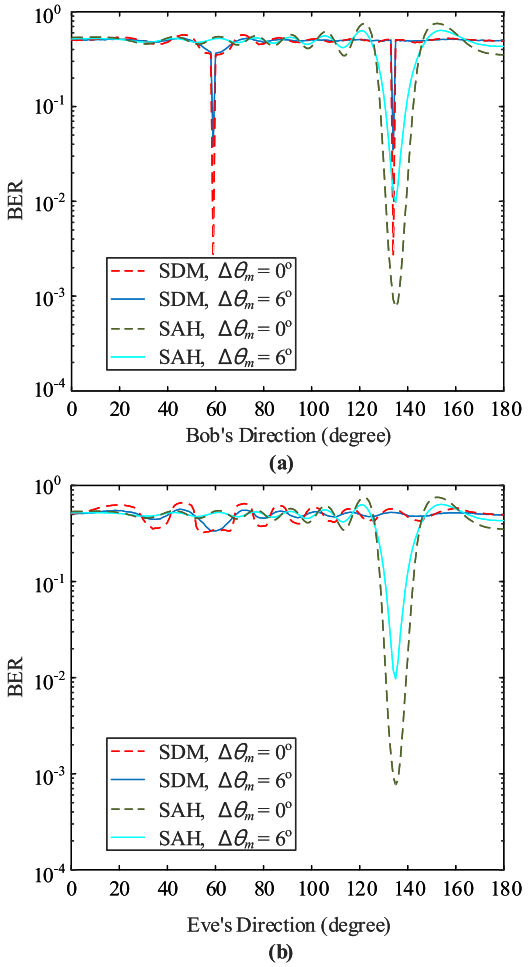

FIGURE 7. BER performance of both the SDM and conventional SAH schemes with and without DME. (a) Bob's BER versus the direction; (b)Eve's BER versus the direction.

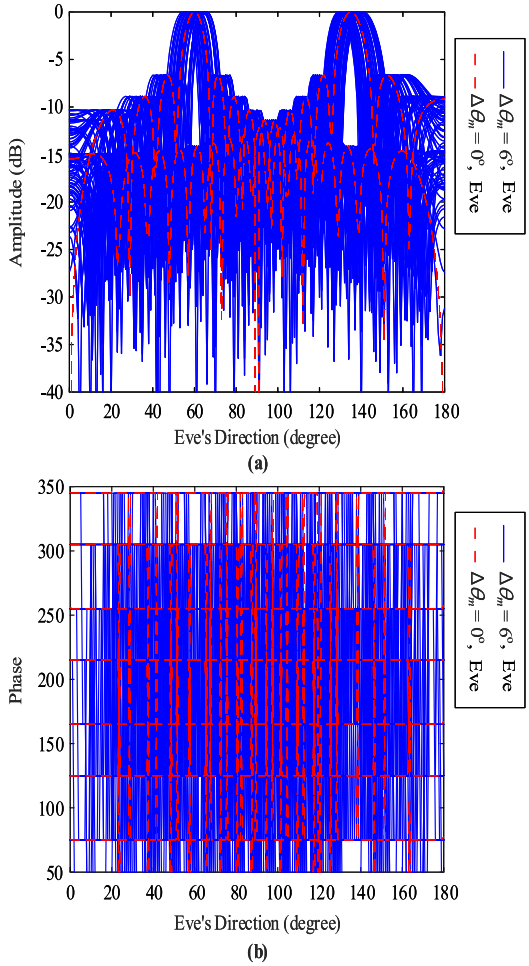

FIGURE 8. Amplitude and phase patterns of the SDM scheme with and without DME. (a) Amplitude pattern versus Eve's direction; (b) Phase pattern versus Eve's direction.

is negligible. This is beneficial in terms of reducing the detection complexity imposed, since the scrambling factor is known at Bob. Furthermore, as observed in Fig. 6(b), Eve's BER performance is poor over the entire maximum DME region. Another important observation is that there exists a distinct gap, which reveals the fact that the SDM scheme is capable of improving the security by the virtue of the scrambling factor. More specifically, for any given

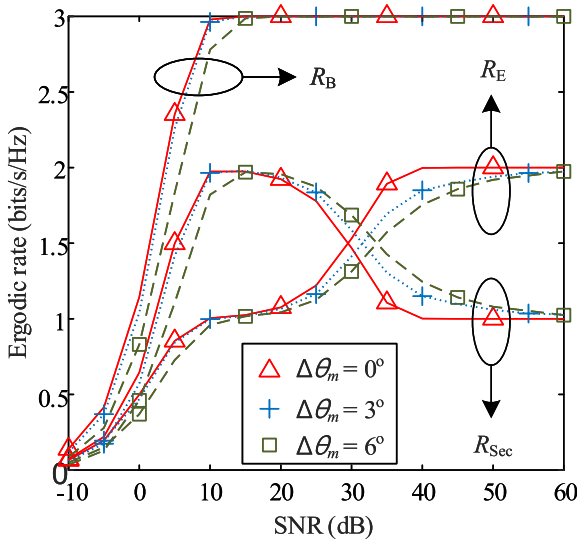

FIGURE 9. Ergodic rates of the SDM system versus the SNR for different maximum DMEs 0°, 3° and 6°.

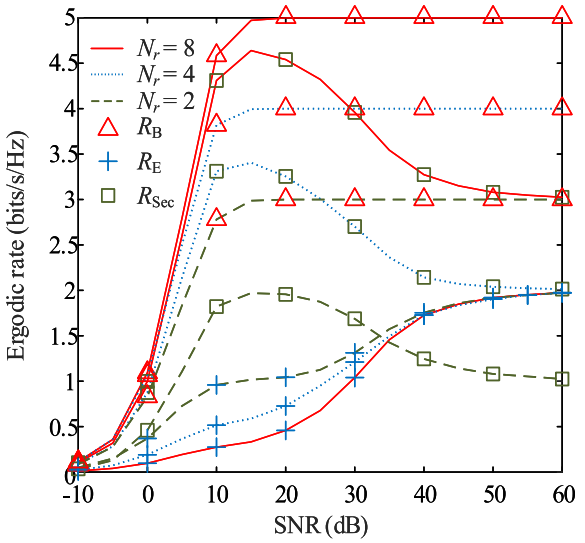

FIGURE 10. Ergodic rates of the SDM system versus the SNR for different Bob's receivers 2, 4 and 8.

value of $\Delta\theta_m$, there exists the same optimal scrambling factor set $\{\alpha_1, \alpha_2\} = \{e^{j180°}, e^{j180°}\}$, which results in the signal constellation subject to phase scrambling 180°.

Fig. 7 illustrates the achievable BER versus the direction for both the SDM and SAH schemes with and without DME, where SNR is fixed to 10dB. It is observed in Fig. 7(a) that Bob's BER performance loss in both SDM and SAH schemes with DME are around 10 times of those without DME. Note that, since more information is transmitted by the index of receivers in the SDM scheme, Bob's BER performance is worse than that of the SAH scheme. By contrast, when Eve and Bob share the same direction, it can be clearly observed in Fig. 7(b) that the SAH scheme can't guarantee secure transmission regardless of the presence of DME, whereas the SDM scheme is insensitive to direction. Hence, compared to conventional SAH, SDM is capable of efficiently preventing the eavesdropping.

Fig. 8 evaluates and compares the amplitude and phase patterns of Eve's received noiseless signal versus Eve's direction for the SDM scheme with and without DME. As can be inferred from Fig. 8, along all Eve's directions, the SDM scheme with DME exhibits severe amplitude and phase scrambling in comparison to the SDM scheme without DME, thanks to the introduction of the scrambling factor and the effect of DME. This implies that the SDM system with DME offers improved security. However, when considering the part of information modulated by the index of the receiver, as observed in Figs. 4-7, the curves change insignificantly at Eve in terms of the BER performance.

B. ERGODIC RATES

Fig. 9 depicts the achievable ergodic rates of Bob and Eve as well as the ergodic secrecy rates of the SDM system versus the SNR, where the effect of DME is also considered. Since the number of cooperative receiver was set to 2, while employing QPSK constellations, Bob reaches the upper bound of 3 bits/s/Hz and Eve reaches the upper bound of 2 bits/s/Hz, when SNR is sufficiently high. Nevertheless, the ergodic secrecy rates first increase until to a peak value, and then decrease to 1 bits/s/Hz, which corresponds to $\log_2 N_r$. On the other hand, as can be observed in Fig. 9, in order to achieve the ergodic rate upper bounds at Bob and Eve, when the maximum DME increases, the required SNR gain also increases. By contrast, the ergodic secrecy rates first decrease to a threshold, and then increase as the maximum DME increases. This is because the fact that the ergodic secrecy rate is the difference between the ergodic rates at Bob and Eve, when Eve's ergodic rate is decreasing, Bob's ergodic rate reaches the upper bound. Furthermore, at a given maximum DME, there exists an optimal SNR for achieving the highest secrecy rate.

Fig. 10 and Fig. 11 respectively show the effect of the number of Bob's receivers N_r and of different APM modulation order M on the ergodic rates for the SDM system, where the maximum DME is fixed to 6°. It can be seen that as expected, higher N_r and higher M yield higher ergodic rate upper bound of $\log_2(MN_r)$ at Bob, and higher M yields higher ergodic rate upper bound of $\log_2 M$ at Eve. Noticeably, when SNR is sufficiently high, the ergodic secrecy rate tends to $\log_2 N_r$, regardless of the value of M. More specially, as shown in Fig. 10, the higher N_r is, the higher the ergodic secrecy rate will be, whereas there is the same optimal SNR for reaching the highest ergodic secrecy rate. Additionally, in Fig. 11, the optimal SNR increases in the medium SNR region, when the modulation order increases. Consequently, both Fig. 10 and Fig. 11 imply that we can improve the highest ergodic secrecy rate by increasing N_r and M. Nevertheless, in practice, it is considerable to increase N_r by increasing the cost of optical fibers and increase M by increasing the complexity of the central unit. Hence, there exists a tradeoff

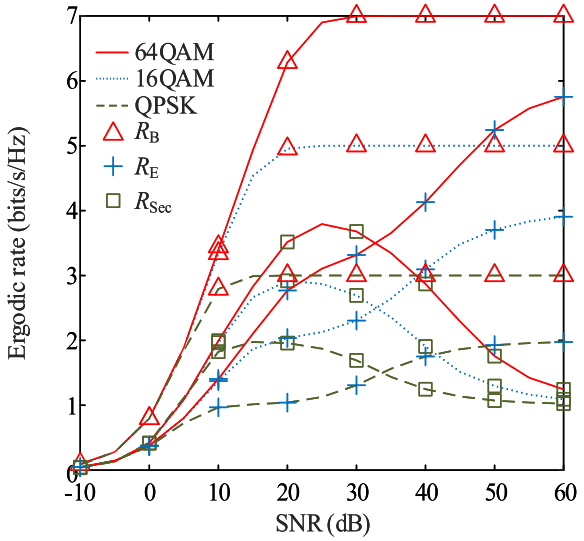

FIGURE 11. Ergodic rates of the SDM system versus the SNR for different APM modulation orders 4, 16 and 64.

among the higher ergodic secrecy rate, the cost of optical fibers and the complexity of central unit.

VI. CONCLUSION

In this contribution, we investigated the impact of IAE on the achievable BER of SDM systems in a practical transmission scenario, and conducted a theoretical analysis in terms of the ABEP union bounds for both Bob and Eve, when ML detector was employed. Moreover, we quantified the ergodic rate with finite alphabet input, when IAE was present. Our simulated results revealed that the derived union bounds are tight. Meanwhile, the BER performance of Bob may be degraded significantly with the increase of the value of the maximum DME. For any given maximum DME, there always exists the same optimal scrambling factor set, which is capable of degrading the performance for Eve, while delivering an achievable performance for Bob. On the other hand, at a given SNR, as the maximum DME increases, the ergodic rates of both Bob and Eve will decrease, whereas the ergodic secrecy rate of the SDM system first decreases to a threshold, and then increases. Furthermore, in order to acheieve the highest ergodic secrecy rate, there always exists an optimal SNR. Our future works will focus on the system design and optimization in the context of multi-path fading channels.

REFERENCES

[1] N. Yang, L. Wang, G. Geraci, M. Elkashlan, J. Yuan, and M. Di Renzo, "Safeguarding 5G wireless communication networks using physical layer security," *IEEE Commun. Mag.*, vol. 53, no. 4, pp. 20–27, Apr. 2015.

[2] P. Yang, Y. Xiao, M. Xiao, and S. Li, "6G wireless communications: Vision and potential techniques," *IEEE Netw.*, vol. 33, no. 4, pp. 70–75, Jul. 2019.

[3] E. G. Larsson, O. Edfors, F. Tufvesson, and T. L. Marzetta, "Massive MIMO for next generation wireless systems," *IEEE Commun. Mag.*, vol. 52, no. 2, pp. 186–195, Feb. 2014.

[4] A. W. Mbugua, W. Fan, Y. Ji, and G. F. Pedersen, "Millimeter wave multi-user performance evaluation based on measured channels with virtual antenna array channel sounder," *IEEE Access*, vol. 6, pp. 12318–12326, 2018.

[5] L. Gupta, R. Jain, and G. Vaszkun, "Survey of important issues in UAV communication networks," *IEEE Commun. Surveys Tuts.*, vol. 18, no. 2, pp. 1123–1152, Nov. 2015.

[6] Y. Gao, H. Ao, Q. Zhou, Z. Feng, W. Zhou, Y. Li, and X. Li, "Modeling of satellite communication systems design with physical layer security," in *Proc. Int. Conf. Wireless Commun. Signal Process. Netw.*, Chennai, India, Mar. 2017, pp. 1680–1683.

[7] S. Popli, R. K. Jha, and S. Jain, "A survey on energy efficient narrowband Internet of Things (NBIoT): Architecture, application and challenges," *IEEE Access*, vol. 7, pp. 16739–16776, 2018.

[8] Y. Ding and V. Fusco, "A review of directional modulation technology," *Int. J. Microw. Wireless Technol.*, vol. 8, no. 7, pp. 1–13, Jul. 2015.

[9] Y. Ding and V. F. Fusco, "Establishing metrics for assessing the performance of directional modulation systems," *IEEE Trans. Antennas Propag.*, vol. 62, no. 5, pp. 2745–2755, May 2014.

[10] M. Hafez and H. Arslan, "On directional modulation: An analysis of transmission scheme with multiple directions," in *Proc. IEEE Int. Conf. Commun. Workshop (ICCW)*, London, U.K., Jun. 2015, pp. 459–463.

[11] F. Shu, Y. Qin, R. Chen, L. Xu, T. Shen, S. Wan, S. Jin, J. Wang, and X. You, "Directional modulation: A secure solution to 5G and beyond mobile networks," 2018, *arXiv:1803.09938*. [Online]. Available: https://arxiv.org/abs/1803.09938

[12] F. Shu, S. Wan, S. Yan, Q. Wang, Y. Wu, R. Chen, J. Li, and J. Lu, "Secure directional modulation to enhance physical layer security in IoT networks," 2017, *arXiv:1712.02104*. [Online]. Available: https://arxiv.org/abs/1712.02104

[13] E. Baghdady, "Directional signal modulation by means of switched spaced antennas," *IEEE Trans. Commun.*, vol. 38, no. 4, pp. 399–403, Apr. 1990.

[14] M. P. Daly and J. T. Bernhard, "Directional modulation technique for phased arrays," *IEEE Trans. Antennas Propag.*, vol. 57, no. 9, pp. 2633–2640, Sep. 2009.

[15] M. P. Daly, E. L. Daly, and J. T. Bernhard, "Demonstration of directional modulation using a phased array," *IEEE Trans. Antennas Propag.*, vol. 58, no. 5, pp. 1545–1550, May 2010.

[16] N. Valliappan, A. Lozano, and R. W. Heath, Jr., "Antenna subset modulation for secure millimeter-wave wireless communication," *IEEE Trans. Commun.*, vol. 61, no. 8, pp. 3231–3245, Aug. 2013.

[17] Y. Ding and V. F. Fusco, "A vector approach for the analysis and synthesis of directional modulation transmitters," *IEEE Trans. Antennas Propag.*, vol. 62, no. 1, pp. 361–370, Jan. 2014.

[18] J. Hu, S. Yan, F. Shu, J. Wang, J. Li, and Y. Zhang, "Artificial-noise-aided secure transmission with directional modulation based on random frequency diverse arrays," *IEEE Access*, vol. 5, pp. 1658–1667, 2017.

[19] Y. Ding and V. Fusco, "Orthogonal vector approach for synthesis of multi-beam directional modulation transmitters," *IEEE Antennas Wireless Propag. Lett.*, vol. 14, pp. 1330–1333, Feb. 2015.

[20] N. N. Alotaibi and K. A. Hamdi, "Switched phased-array transmission architecture for secure millimeter-wave wireless communication," *IEEE Trans. Commun.*, vol. 64, no. 3, pp. 1303–1312, Mar. 2016.

[21] Y. Xiao, W. Tang, Y. Xiao, H. Zhang, G. Wu, and W. Xiang, "Directional modulation with cooperative receivers," *IEEE Access*, vol. 6, pp. 34992–35000, 2018.

[22] Q. D. You and Y. P. Xiao, "Spatial and directional modulation with scrambling," *Phys. Commun.*, vol. 35, Aug. 2019, Art. no. 100694.

[23] R. Y. Mesleh, H. Haas, S. Sinanovic, C. W. Ahn, and S. Yun, "Spatial modulation," *IEEE Trans. Veh. Technol.*, vol. 57, no. 4, pp. 2228–2241, Jul. 2008.

[24] S. Sugiura and L. Hanzo, "Effects of channel estimation on spatial modulation," *IEEE Signal Process. Lett.*, vol. 19, no. 12, pp. 805–808, Dec. 2012.

[25] R. Zhang, L.-L. Yang, and L. Hanzo, "Generalised pre-coding aided spatial modulation," *IEEE Trans. Wireless Commun.*, vol. 12, no. 11, pp. 5434–5443, Nov. 2013.

[26] X.-Q. Jiang, M. Wen, H. Hai, J. Li, and S. Kim, "Secrecy-enhancing scheme for spatial modulation," *IEEE Commun. Lett.*, vol. 22, no. 3, pp. 550–553, Dec. 2017.

[27] C. Rusu, N. Gonzalez-Prelcic, and R. W. Heath, Jr., "An attack on antenna subset modulation for millimeter wave communication," in *Proc. IEEE Int. Conf. Acoust. Speech Signal Process.*, Brisbane, QLD, Australia, Apr. 2015, pp. 2914–2918.

[28] J. S. Hu, F. Shu, and J. Li, "Robust synthesis method for secure directional modulation with imperfect direction angle," *IEEE Commun. Lett.*, vol. 20, no. 6, pp. 1084–1087, Jun. 2016.

[29] F. Shu, X. Wu, J. Li, R. Chen, and B. Vucetic, "Robust synthesis scheme for secure multi-beam directional modulation in broadcasting systems," *IEEE Access*, vol. 6, pp. 6614–6623, 2016.
[30] F. Shu, W. Zhu, X. Zhou, J. Li, and J. Lu, "Robust secure transmission of using main-lobe-integration-based leakage beamforming in directional modulation MU-MIMO systems," *IEEE Syst. J.*, vol. 12, no. 4, pp. 3775–3785, 2017.
[31] F. Shu, L. Xu, J. Wang, W. Zhu, and Z. Xiaobo, "Artificial-noise-aided secure multicast precoding for directional modulation systems," *IEEE Trans. Veh. Technol.*, vol. 67, no. 7, pp. 6658–6662, Jul. 2018.
[32] D. Castanheira and A. Gameiro, "Distributed antenna system capacity scaling [coordinated and distributed MIMO]," *IEEE Wireless Commun.*, vol. 17, no. 3, pp. 68–75, Jun. 2010.
[33] Y. Zhao, X. Su, J. Zeng, Y. You, and X. Xu, "Capacity analysis and antenna selection strategy for multi-user distributed antenna system," in *Proc. 11th Int. Conf. ITS Telecommun.*, St. Petersburg, Russia, Aug. 2011, pp. 1–4.
[34] H. Ishikawa and Y. Sanada, "System throughput analysis on using joint detection in distributed antenna system," in *Proc. IEEE 88th Veh. Technol. Conf. (VTC-Fall)*, Chicago, IL, USA, Aug. 2018, pp. 1–5.
[35] Q. Cheng, "Directional modulation aided secure spatial modulation," in *Proc. Int. Conf. Mech., Electr., Electron. Eng. Sci. (MEEES)*, Guilin, China, May 2018, pp. 1–7.
[36] M. Bloch, J. Barros, M. R. D. Rodrigues, and S. W. McLaughlin, "Wireless information-theoretic security," *IEEE Trans. Inf. Theory*, vol. 54, no. 6, pp. 2515–2534, Jun. 2008.
[37] R. Zhang, L.-L. Yang, and L. Hanzo, "Error probability and capacity analysis of generalised pre-coding aided spatial modulation," *IEEE Trans. Wireless Commun.*, vol. 14, no. 1, pp. 364–375, Jan. 2015.
[38] X. Guan, Y. Cai, and W. Yang, "On the secrecy mutual information of spatial modulation with finite alphabet," in *Proc. Int. Conf. Wireless Commun. Signal Process. (WCSP)*, Huangshan, China, Oct. 2012, pp. 1–4.

HONGYAN ZHANG received the B.S. degree in communication engineering from the University of Electronic Science and Technology of China (UESTC), in 2018, where she is currently pursuing the M.S. degree with the National Key Laboratory of Science and Technology on Communications. Her research interest is in signal processing toward future wireless communication systems.

YUE XIAO received the Ph.D. degree in communication and information systems from the University of Electronic Science and Technology of China (UESTC), in 2007. He is currently a Professor with the National Key Laboratory of Science and Technology on Communications, UESTC. He has published more than 100 international journals and has been in charge of more than 20 projects in the area of Chinese 3G/4G/5G wireless communication systems. He is also an Inventor of more than 50 Chinese and PCT patents on wireless systems. His research interest is in system design and signal processing toward future wireless communication systems. He currently serves as an Associate Editor for the IEEE COMMUNICATIONS LETTERS.

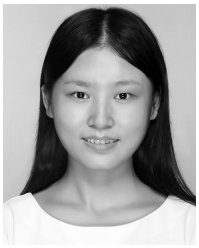

YANPING XIAO received the B.S. degree in communication engineering from the University of Electronic Science and Technology of China (UESTC), in 2015, and the M.S. degree from the National Key Laboratory of Science and Technology on Communications, UESTC, in 2019. Her research interest is in signal processing toward future wireless communication systems.

WEI XIANG received the B.Eng. and M.Eng. degrees in electronic engineering from the University of Electronic Science and Technology of China, Chengdu, China, in 1997 and 2000, respectively, and the Ph.D. degree in telecommunications engineering from the University of South Australia, Adelaide, Australia, in 2004. From 2004 to 2015, he was with the School of Mechanical and Electrical Engineering, University of Southern Queensland, Toowoomba, Australia. In 2008, he was a Visiting Scholar with Nanyang Technological University, Singapore. From October 2010 to March 2011, he was a Visiting Scholar with the University of Mississippi, Oxford, MS, USA. From August 2012 to March 2013, He was an Endeavour Visiting Associate Professor with The University of Hong Kong. He is currently a Foundation Professor and the Head of the electronic systems and internet of things engineering with the College of Science and Engineering, James Cook University, Cairns, Australia. He has published over 160 articles in peer-reviewed journal and conference papers. His research interests are in the broad area of communications and information theory, particularly coding and signal processing for multimedia communications systems. He is a Fellow of IET and Engineers Australia. He was a co-recipient of three Best Paper Awards at 2015 WCSP, 2011 IEEE WCNC, and 2009 ICWMC. He has been awarded several prestigious fellowship titles. He was named a Queensland International Fellow by the Queensland Government of Australia, from 2010 to 2011, an Endeavour Research Fellow by the Commonwealth Government of Australia, from 2012 to 2013, a Smart Futures Fellow by the Queensland Government of Australia, from 2012 to 2015, and a JSPS Invitational Fellow jointly by the Australian Academy of Science and Japanese Society for Promotion of Science, from 2014 to 2015. He is also an Editor of the IEEE COMMUNICATIONS LETTERS.